As originally published in the IPC APEX EXPO Proceedings.

Drop Test Performance of Bga Assembly Using Sac105ti Solder Spheres

Weiping Liu and Ning-Cheng Lee
Indium Corporation
Clinton, NY
Simin Bagheri, Polina Snugovesky, Jason Bragg, Russell Brush, and Blake Harper
Celestica International Inc.
Toronto, Ontario

Abstract
Board-level drop test performance was evaluated and compared for the following four different solder combinations in BGA/CSP assembly: 1) SnPb paste with SnPb balls, 2) SnPb paste with SAC105Ti balls, 3) SAC305 paste with SAC105Ti balls, and 4) SAC305 paste with SAC105 balls. The presence of Ti improved the drop test performance significantly, despite the voiding side effect caused by its oxidation tendency. It is anticipated that the voiding can be prevented with the development of a more oxidation resistant flux. The consistently poor drop test performance of 105Ti/SnPb is caused by the wide pasty range resulting from mixing SAC105Ti with Sn63 solder paste. The effect of Ti in this system is overshadowed by the high voiding outcome due to this wide pasty range material. In view of this, the use of a SAC105 BGA with an SnPb solder paste is not recommended, with or without the Ti addition. High reflow temperatures drove the fracture to shift to the interface at the package side, presumably through building up the IMC thickness beyond the threshold value. A lower reflow temperature is recommended. The electrical response is consistent with the complete fracture data, but the complete fracture trend is inconsistent with that of the partial fracture trend, and neither data can provide a full understanding about the failure mode. By integrating the complete fracture and the partial fracture into a "Virtual Fracture", the failure mechanism becomes obvious and data sets become consistent with each other.

Introduction
Driven by environmental considerations, the electronics industry has been migrating toward lead-free soldering since the late 1990s. Presently, the prevailing solder alloys are mainly SnAgCu (SAC) alloys with high silver content, such as Sn3.8Ag0.7Cu (SAC387) and Sn3.0Ag0.5Cu (SAC305). Although high Ag SAC alloys are widely adopted, the fragility of solder joints of area array packages, such as BGAs or CSPs, causes major concern for portable devices. Low Ag SAC alloys such as SAC105 are proposed as a solution, but with only limited success. Other alloys such as SAC alloys modified with a variety of additives are also attempted. Again, the outcome is mixed. Among those promising new materials, Ti has been reported as a very effective dopant to SAC alloy for improvement of drop test performance in a simplified simulation study [1]. In this work, BGA solder spheres using SAC105 with 0.02% addition of Ti (SAC105Ti) were evaluated for BGA assembly drop test performance. The results will be presented and discussed below.

Experimental
1. Materials

The following alloy combinations were tested in this work, as shown in Table 1. No-clean flux chemistry and type 3 powder were used for both Sn63 and SAC305 solder pastes.

Table 1 - Solder alloys used for solder sphere and solder paste.

Set	Solder sphere	Solder paste
1	Sn63	Sn63
2	SAC105Ti	Sn63
3	SAC105Ti	SAC305
4	SAC105	SAC305

2. Test Components

Three area array packages were used in this study, as shown in Table 2. In this work, SAC105Ti and SAC105 BGAs were made by reballing from previous SAC305 BGAs. Also, BGA256 is a perimeter array, while BGA196 is full array.

Table 2 - Area array packages used in this study.

Package type	Body size (mm)	Sphere diameter (mm)	Pitch (mm)	I/O
BGA256	27	0.76	1.27	256
BGA196	15	0.5	1.0	196
CSP64	8	0.46	0.8	64

3. Test Vehicle

The test vehicle is made of Laminate Polyclad FR370HR material, 8" x 10" in size, with SMD pads and OSP surface finish. The board material has a T_g of 180°C and a decomposition temperature of 350°C, which provides tolerance toward lead free reflow temperatures. Two components of each type were incorporated on the test board, with a total of 6 components on each board, as shown in Figure 1.

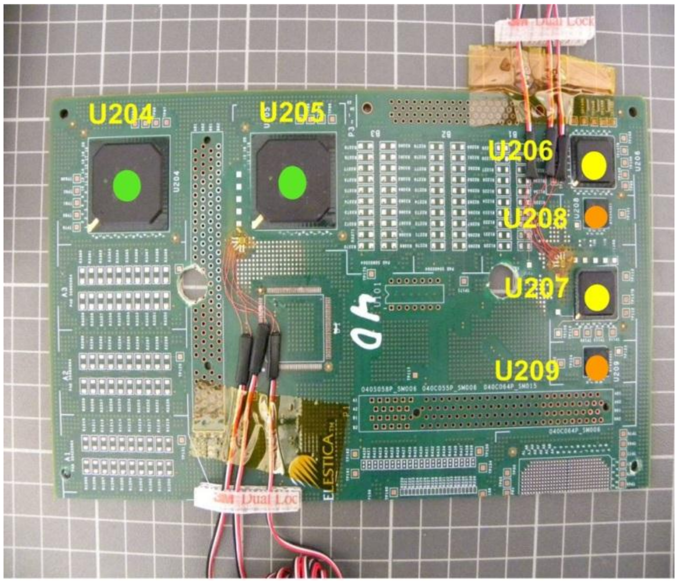

Figure 1 - Test vehicle layout, with two BGA256 (U204, U205, in green), two BGA196 (U206, U207, in yellow), and two CSP64 (U208, U209, in orange) located on the board.

4. Test Matrix

For drop test, 5 boards were tested for each set of the four alloy combinations shown in Table 1. Overall, 20 boards were tested for drop test.

5. Reflow Profile

After solder paste printing and component placement, the board was reflowed with a 10-zone forced air convection oven under air. For SAC305 paste assembly, profile 1 (see Figure 2) was employed, with peak temperature 235 +3 ºC, and 90±10 seconds above 217 ºC. For SnPb (Sn63) paste assembly, profile 2 (see Figure 3) was employed, with peak temperature 230+3 ºC, and 60±10 seconds above 183 ºC.

6. Drop Test

This board-level drop test is based on the JEDEC Standard JESD22-B110A known as Subassembly Mechanical Shock Test. The shock parameters are 1500 G, with 0.5 ms duration. All cards were put through 100 drops, with 1 board tested at a time, and 20 boards in total. Two 220g weights were added to cards to increase strain and help induce solder failures. One board from each batch was monitored on 2 drops for shock input (with an accelerometer mounted to the board) and board strain. Each board was monitored in-situ for resistance changes. The first failure determined for each location is recorded as the number of drops to failure. If no failure is observed after 100 drops, the number is entered as 101.

7. Dye and Pry Test

After 100 drops were completed on all cards, the tested cards were immersed in red dye and subjected to a vacuum to force the dye into the pre-existing cracks caused by drop testing. The dye was then cured and the parts were pried off the board to inspect the failure modes**.**

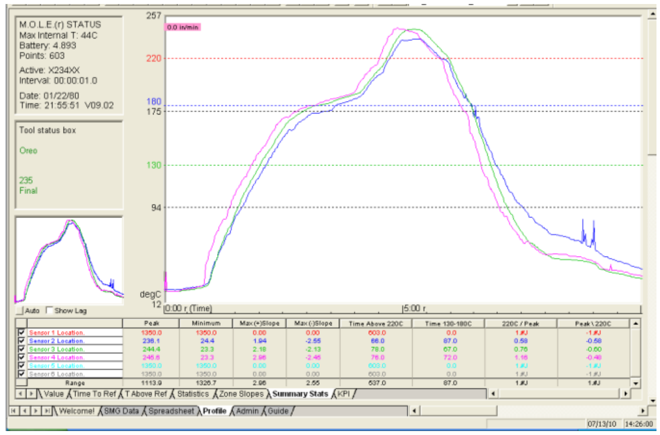

Figure 2 - Reflow profile 1, with peak temperature 235+3 ºC, and 90±10 seconds above 217 ºC.

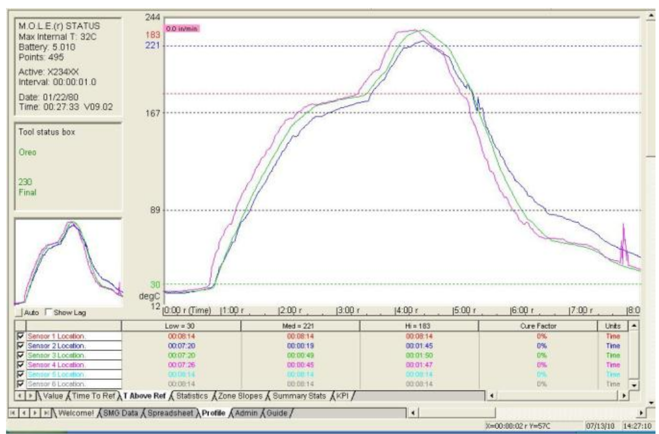

Figure 3 - Reflow profile 2, with peak temperature 230+3 ºC, and 60±10 seconds above 183 ºC.

Results

1. Drop Test Electrical Response

BGA256

The test results on BGA256 are tabulated in Table 4 for components located at corner (U204) and at edge (U205).

BGA196

The test results on BGA196 are tabulated in Table 5 for components located at corner (U206) and at edge (U207).

CSP64

The test results on CSP64 are tabulated in Table 6 for components located near corner (U208) and at edge (U209).

Overall Average

The average value of drop test performance shown in Table 4 to Table 6 is compiled in Table 7, with overall average calculated. The ranking of overall electrical continuity performance is: SnPb/SnPb ball (best) > SAC305/SAC105Ti ball > SAC305/SAC105 ball > SnPb/SAC105Ti ball.

2. Dye and Pry Test

At dye and pry test, the failures are categorized as complete fracture or partial fracture. Fig. 4 shows results of dye and pry test with complete fractures, while Fig. 5 shows results with partial fractures. All data presented is average of 5 boards.

When only complete fracture is considered, as shown in Figure 4, the drop failure resistance ranking is: SnPb/SnPb ball (best) > SAC305/SAC105Ti ball > SAC305/SAC105 balls > SnPb/SAC105Ti ball.
When only partial fracture is considered, as shown in Figure 5, the drop failure resistance ranking is: SAC305/SAC105Ti ball (best) > SAC305/SAC105 ball > SnPb/SAC105Ti ball > SnPb/SnPb ball.

Table 4 - Drop test results for U204 and U205 (BGA256) locations

Event Detector

U204	SnPb SnPb	SnPb 105Ti	SAC305 105Ti	SAC305 105
1	41	61	44	14
2	45	28	101	56
3	59	35	44	33
4	62	24	101	58
5	62	57	60	96
Maximum	62	61	101	96
Minimum	41	24	44	14
Average	53.8	41	70.0	51.4
Standard Deviation	10	17	29	31

Event Detector

U205	SnPb SnPb	SnPb 105Ti	SAC305 105Ti	SAC305 105
1	18	16	18	11
2	8	16	43	13
3	27	13	21	16
4	1	11	19	11
5	17	15	33	15
Maximum	27	16	43	16
Minimum	1	11	18	11
Average	14.2	14.2	26.8	13.2
Standard Deviation	10	2	11	2

Table 5 - Drop test results for U206 and U207 (BGA196) locations

Event Detector

U206	SnPb SnPb	SnPb 105Ti	SAC305 105Ti	SAC305 105
1	101	54	101	101
2	101	22	101	101
3	101	8	101	52
4	101	31	101	101
5	101	101	101	101
Maximum	101	101	101	101
Minimum	101	8	101	52
Average	101	43.2	101	91.2
Standard Deviation	0	36	0	22

Event Detector

U207	SnPb SnPb	SnPb 105Ti	SAC305 105Ti	SAC305 105
1	101	53	101	49
2	101	55	62	52
3	101	18	101	101
4	101	22	101	101
5	101	13	101	101
Maximum	101	55	101	101
Minimum	101	13	62	49
Average	101	32.2	93	80.8
Standard Deviation	0	20	17	28

Table 6 - Drop test results for U208 and U209 (CSP64) locations

Event Detector

U208	SnPb SnPb	SnPb 105Ti	SAC305 105Ti	SAC305 105
1	101	47	101	101
2	101	101	27	13
3	101	101	57	101
4	101	101	101	10
5	101	92	101	101
Maximum	101	101	101	101
Minimum	101	47	27	10
Average	101	88.4	77	65.2
Standard Deviation	0	23	34	49

Event Detector

U209	SnPb SnPb	SnPb 105Ti	SAC305 105Ti	SAC305 105
1	101	101	2	14
2	101	6	19	2
3	101	13	101	12
4	101	101	101	85
5	101	101	79	3
Maximum	101	101	101	85
Minimum	101	6	2	2
Average	101	64.4	60	23.2
Standard Deviation	0	50	47	35

Table 7 - Average of drop test performance.

Parts	SnPb/SnPb	105Ti/SnPb	105Ti/305	105/305
U204	53.8	41	70	51.4
U205	14.2	14.2	26.8	13.2
U206	101	43.2	101	91.2
U207	101	32.2	93	80.8
U208	101	88.4	77	65.2
U209	101	64.4	60	23.2
Average	78.7	47.2	71.3	54.2

Which Is Better?

1. Electrical or Fracture Response

Electrical Correlates with Complete Fracture

The trend on the number of interconnects with complete fractures after 100 drops in each component and cell (Figure 4) matches the trend of electrical testing results in terms of the number of drops to first failure (Table 7). This close correlation reflects that the causes of the two failure types are fairly similar. Since electrical failure can only be caused by complete fracture, the mechanism which caused the first electrical failure, or first complete fracture, continued on causing more complete fractures after 100 drops. Alloy combinations, which are more prone to have a first complete fracture, also display more complete fractures after 100 drops.

Partial Fracture No Correlation

The trend on the number of partial fractures on each component (Figure 5) does not match the trend of electrical drop testing results, since there was no change in electrical resistance, due to only partial interconnect failures.

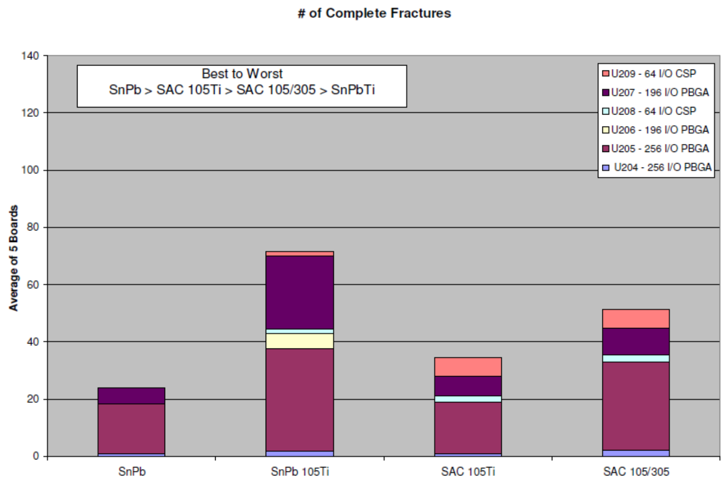

Figure 4 - Results of dye and pry test with complete fractures. Data presented is average of 5 boards.

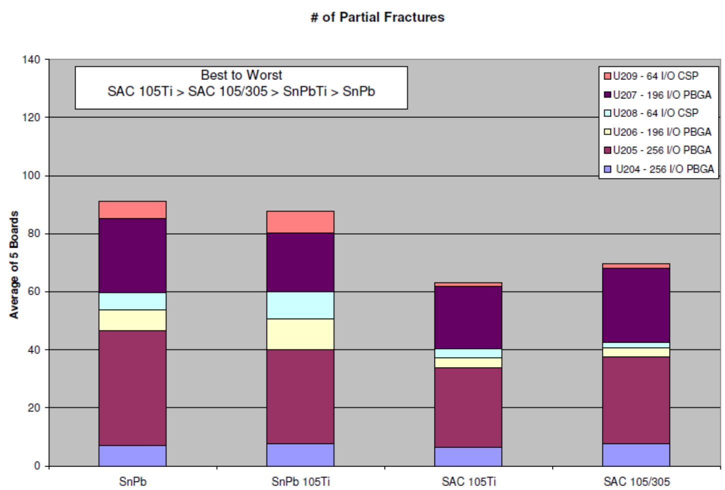

Figure 5 - Results of dye and pry test with partial fractures. Data presented is average of 5 boards.

No Insight Out of Electrical

By examining Table 7, the relative fracture resistance of alloy combinations varies with component type. No more electrical test data is available for interpreting the significance of this component type sensitivity. This strongly suggests that electrical testing is not informative enough in understanding the effect of alloy combinations. Dye and pry tests may provide a deeper insight about the material performance.

Combined Fracture Data Desired

In the dye and pry test, a complete fracture does not reflect a partial fracture, including board cratering, thus is not representative of the potential of drop fracture resistance of alloy combinations. The fact that Figure 4 and Figure 5 exhibit different relative drop fracture resistance of alloy combinations indicates neither fracture mode can represent the potential of alloy combinations.

Since both complete and partial fractures reflect damages associated with certain alloy combination, the potential of alloy combinations toward drop fracture resistance should consider both fracture modes of the dye and pry test. Figure 6 shows the interconnect fracture modes defined in IPC/JEDEC-9702. Table 8 shows the crack sites determined in the dye and pry test on all area array packages tested. In this table, a partial crack is noted with a * mark on the site number associated.

Table 8 - Dye and pry test results on BGA256, BGA196, and CSP64

BGA256	Fracture Type	204 (1)	204 (2)	204 (3)	204 (4)	204 (5)	205 (1)	205 (2)	205 (3)	205 (4)	205 (5)	Total
SnPb/SnPb	Top (5)	0	0	0	0	0	0	0	0	0	0	0
	Top (3*)	0	0	0	0	0	0	0	0	0	0	0
	Top (3)	0	0	0	0	0	0	0	0	0	0	0
	Bottom (8*)	0	0	0	0	0	0	0	0	0	0	0
	Bottom (8)	0	0	0	0	0	0	0	0	0	0	0
	Bottom (10*)	11	12	5	5	6	52	43	39	41	21	235
	Bottom (10)	3	0	0	1	1	12	10	13	20	32	92
105Ti/SnPb	Top (5)	0	0	0	0	0	0	0	0	1	1	2
	Top (3*)	0	1	0	0	0	2	1	1	3	2	10
	Top (3)	0	0	0	0	0	5	0	1	5	5	16
	Bottom (8*)	0	3	0	0	1	5	12	1	3	14	39
	Bottom (8)	0	0	0	0	0	5	3	7	11	12	38
	Bottom (10*)	4	9	4	5	12	16	37	16	24	21	148
	Bottom (10)	0	4	4	1	0	13	28	24	20	39	133
105Ti/305	Top (5)	0	0	0	0	0	0	0	0	0	0	0
	Top (3*)	0	0	0	0	0	0	0	0	0	0	0
	Top (3)	0	0	0	0	0	0	0	0	0	0	0
	Bottom (8*)	0	0	0	0	0	0	1	0	0	0	1
	Bottom (8)	0	0	0	0	0	0	1	0	0	0	1
	Bottom (10*)	13	6	2	5	6	33	24	32	29	18	168
	Bottom (10)	1	0	0	0	3	26	19	19	14	11	93
105/305	Top (5)	0	0	0	0	0	0	0	0	0	0	0
	Top (3*)	0	0	0	0	0	0	0	0	0	0	0
	Top (3)	0	0	0	0	0	0	0	0	0	0	0
	Bottom (8*)	0	0	1	0	0	0	2	0	0	1	4
	Bottom (8)	0	0	0	0	0	1	3	0	1	0	5
	Bottom (10*)	6	6	8	14	3	30	29	37	24	28	185
	Bottom (10)	0	0	0	11	0	37	29	31	35	14	157
BGA196	Fracture Type	206 (1)	206 (2)	206 (3)	206 (4)	206 (5)	207 (1)	207 (2)	207 (3)	207 (4)	207 (5)	Total
SnPb/SnPb	Top (5)	0	0	0	0	0	0	0	0	0	0	0
	Top (3*)	0	0	1	0	0	0	0	0	0	0	1
	Top (3)	0	0	0	0	0	0	1	0	0	0	1
	Bottom (8*)	0	0	1	0	0	0	0	0	1	0	2
	Bottom (8)	0	0	0	0	0	0	0	0	0	0	0
	Bottom (10*)	10	21	0	0	3	29	19	28	26	24	160
	Bottom (10)	0	0	0	0	0	1	24	0	0	2	27
105Ti/SnPb	Top (5)	0	0	0	0	0	0	0	0	0	0	0
	Top (3*)	1	3	0	4	2	3	3	0	4	14	34
	Top (3)	5	7	0	2	3	7	7	14	25	2	72
	Bottom (8*)	0	9	0	15	7	12	3	2	4	15	67
	Bottom (8)	4	3	0	1	0	14	1	10	29	1	63
	Bottom (10*)	2	2	1	5	0	5	18	4	3	8	48
	Bottom (10)	1	0	0	0	0	2	8	1	5	1	18
105Ti/305	Top (5)	0	0	0	0	0	0	0	0	0	0	0
	Top (3*)	0	0	0	0	2	0	0	0	7	0	9
	Top (3)	0	0	0	0	0	0	0	0	1	1	2
	Bottom (8*)	0	0	0	0	0	2	3	0	0	0	5
	Bottom (8)	0	0	0	0	0	0	0	0	0	1	1
	Bottom (10*)	4	4	2	3	2	35	16	0	30	14	110
	Bottom (10)	0	0	0	0	0	4	8	0	21	2	35
105/305	Top (5)	0	0	0	0	0	0	0	0	0	0	0
	Top (3*)	0	0	0	1	1	1	0	1	7	2	13
	Top (3)	0	0	0	0	0	3	0	1	1	1	6
	Bottom (8*)	1	0	0	0	1	1	2	1	2	2	10
	Bottom (8)	0	0	0	0	0	3	0	2	1	0	6
	Bottom (10*)	3	5	4	0	0	12	39	15	26	16	120
	Bottom (10)	0	1	0	0	0	4	8	2	17	4	36
CSP64	Fracture Type	208 (1)	208 (2)	208 (3)	208 (4)	208 (5)	209 (1)	209 (2)	209 (3)	209 (4)	209 (5)	Total
SnPb/SnPb	Top (5)	0	0	0	0	0	0	0	0	0	0	0
	Top (3*)	0	0	0	0	0	0	0	0	0	0	0
	Top (3)	0	0	0	0	0	0	0	0	0	0	0
	Bottom (8*)	6	12	2	6	4	5	7	4	10	4	60
	Bottom (8)	0	0	0	0	0	0	0	0	0	0	0
	Bottom (10*)	0	0	0	0	0	0	0	0	0	0	0
	Bottom (10)	0	0	0	0	0	0	0	0	0	0	0
105Ti/SnPb	Top (5)	0	0	0	0	0	0	0	0	0	0	0
	Top (3*)	1	0	0	0	1	0	6	0	2	4	14
	Top (3)	3	0	0	0	0	1	4	0	0	0	8
	Bottom (8*)	6	11	2	17	8	1	3	4	12	2	66
	Bottom (8)	2	0	4	0	0	4	0	1	1	0	12
	Bottom (10*)	0	0	0	0	0	0	0	0	0	0	0
	Bottom (10)	0	0	0	0	0	0	0	0	0	0	0
105Ti/305	Top (5)	0	0	0	0	0	0	0	0	0	0	0
	Top (3*)	1	0	0	0	3	0	0	2	1	1	8
	Top (3)	1	4	0	4	0	22	2	2	3	4	42
	Bottom (8*)	2	0	0	0	0	0	2	0	0	1	5
	Bottom (8)	0	0	0	0	0	0	1	0	0	0	1
	Bottom (10*)	0	0	10	0	0	0	0	0	0	0	10
	Bottom (10)	0	0	3	0	0	0	0	0	0	0	3
105/305	Top (5)	0	0	0	0	0	0	0	0	0	0	0
	Top (3*)	1	0	0	3	0	3	3	0	2	3	15
	Top (3)	5	0	3	2	0	18	0	2	2	6	38
	Bottom (8*)	0	2	0	0	3	0	0	1	0	0	6
	Bottom (8)	0	1	1	0	0	0	0	0	0	1	3
	Bottom (10*)	0	0	0	0	0	0	0	0	0	0	0
	Bottom (10)	0	0	0	0	0	0	0	0	0	0	0
Note:	* partial fracture											
	(blue)	resin fracture		(yellow)	solder fracture							

2. Integrating Fracture Data

Virtual Fracture

Every individual complete fracture is assigned as “one” fracture. On the other hand, since partial fracture may range from nearly no fracture to nearly complete fracture, the median value 0.5 is adopted for every partial fracture. The total amount of the virtual fracture for each type of package/alloy combination is the sum of complete fracture and partial fracture. For instance, a system with 7 complete fractures and 10 partial fractures is regarded as having 7 + 10 x 0.5 = 12 virtual fractures.

Table 9 - Total number of solder joints tested in dye & pry test.

Package	SnPb/SnPb	105Ti/SnPb	105Ti/305	105/305
BGA256	2560	2560	2560	2560
BGA196	1960	1960	1960	1960
CSP64	640	640	640	640

Normalizing Virtual Fracture

In this study, 10 packages were analyzed for a dye and pry test for each package type and alloy combination. Table 9 shows the total number of solder joints tested in dye and pry tests for each system. For each system, the fracture is normalized by dividing the virtual fracture by the total number of joints tested. Table 10 shows the normalized virtual fracture of the systems studied. The fracture sites listed in Table 10 is illustrated in Figure 7.

Table 10 - Normalized virtual fracture of systems tested in dye and pry test.

Package	Fracture site	SnPb/SnPb	105Ti/SnPb	105Ti/305	105/305
BGA256	Top (resin)	0.0%	0.1%	0.0%	0.0%
	Top (interface)	0.0%	0.8%	0.0%	0.0%
	Bottom (interface)	0.0%	2.2%	0.1%	0.3%
	Bottom (resin)	8.2%	8.1%	6.9%	9.7%
BGA196	Top (resin)	0.0%	0.0%	0.0%	0.0%
	Top (interface)	0.1%	4.5%	0.3%	0.6%
	Bottom (interface)	0.1%	4.9%	0.2%	0.6%
	Bottom (resin)	5.5%	2.1%	4.6%	4.9%
CSP64	Top (resin)	0.0%	0.0%	0.0%	0.0%
	Top (interface)	0.0%	2.3%	7.2%	7.1%
	Bottom (interface)	4.7%	7.0%	0.5%	0.9%
	Bottom (resin)	0.0%	0.0%	1.3%	0.0%

Note 1. Partial fracture = 0.5 fracture

2. Failure expressed as percentage of overall solder joints

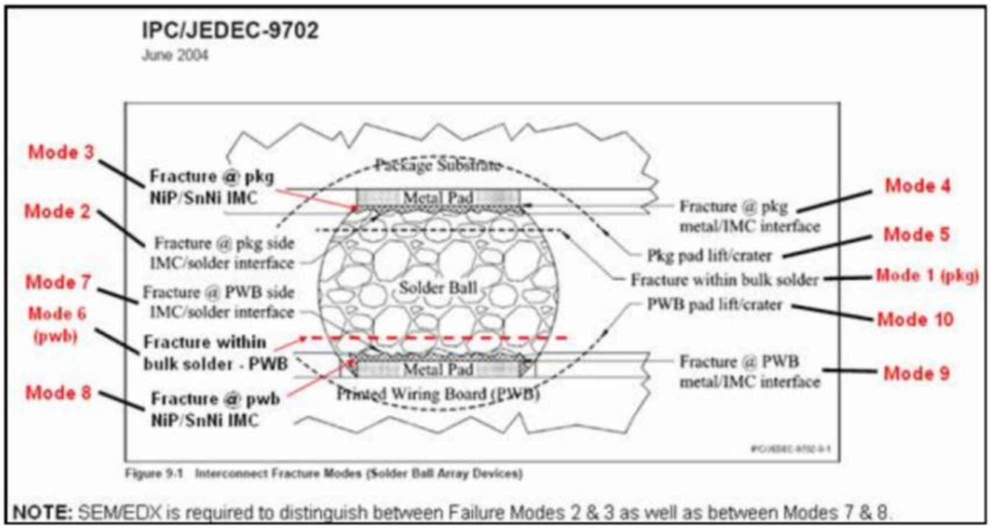

Figure 6 - Interconnect fracture modes (solder ball array device) IPC/JEDEC-9702.

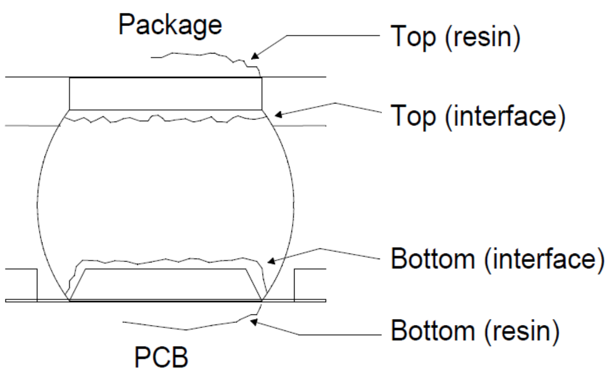

Figure 7 - Failure sites shown in Table 10.

Failure Analysis

1. Effect of Package Size

The size of the three packages is shown in Table 2, with the size decreases in the order: BGA256 > BGA196 > CSP64. With all components located around the perimeter of the board, as shown in Figure 1, it is reasonable to expect the solder joint temperature of the packages at reflow to decrease in the following order: CSP64 > BGA196 > BGA256. This is evidenced by the observation that the microstructure of CSP64 is more uniform than BGA256 for 105Ti/SnPb paste system at the same oven setting, as shown in Figure 8.

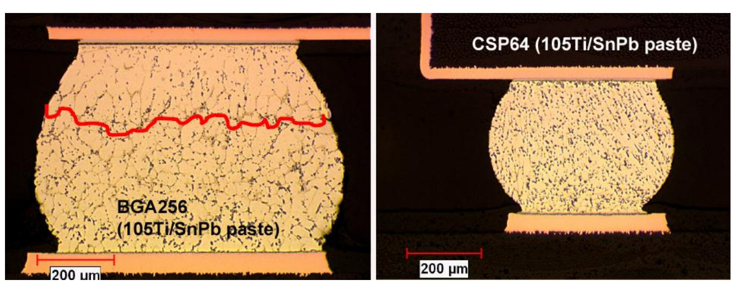

Figure 8 - Microstructure of BGA256 and CSP64 (SAC105Ti/SnPb paste) with the same profile setting.

Figure 9 is derived from Table 10. It shows that with decreasing package size, the resin fracture decreases and the interface fracture increases. The increasing interface fracture can be attributed to the increasing intermetallic formation due to a higher reflow temperature for a smaller package. Table 11 summarizes the relation between package size and fracture location.

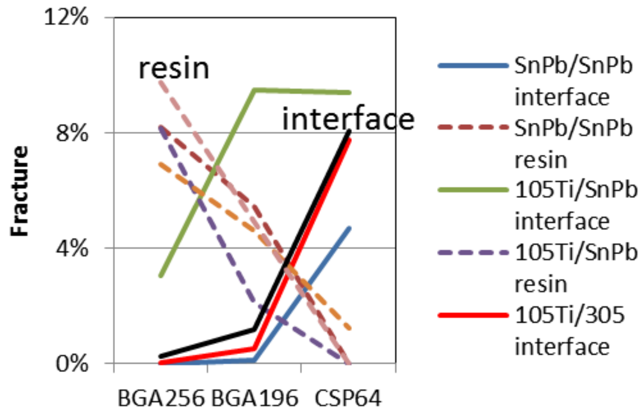

Figure 9 - Effect of package type on fracture

Table 11 – Effect of package size on fracture behavior

Package	SnPb/SnPb	105Ti/SnPb	105Ti/305	105/305
BGA256 (27mm, 0.76mm ball)				
BGA196 (15mm, 0.5mm ball)				
CSP64 (8mm, 0.46mm ball)		Hotter Joint (smaller chip) cause more interface failure.		

2. Effect of Pasty Range and Ti

Excessive voiding was observed for both 105Ti/SnPb and 105Ti/305 solder joints, particularly in the case of 105Ti/SnPb. The excessive voiding associated with the assembly of SAC105 BGA with SnPb solder paste has been reported by Henshall et al. [2,3], and was attributed to the 47°C wide pasty range (177°C to 224°C) of the alloy mixture. Since SAC105Ti is virtually identical with SAC105 in melting range [1], 105Ti/SnPb paste is also expected to have a similarly wide pasty range and the resultant excessive voiding. This excessive voiding caused by a wide pasty range is considered the root cause of an excessively high fracture rate among all alloy combinations. In this case, the presence of Ti is estimated to have at most a minute effect.

105Ti/305 was observed to have more voiding than 105/305. This is attributed to the relatively high oxidation tendency of Ti, as illustrated by the Gibbs free energy of metal oxide formation of several metals at ambient condition [4], as shown in Table 12.

However, despite this unfavorable effect of oxidation, 105Ti/305 still exhibits a lower overall fracture rate compared with 105/305, and is even lower than SnPb/SnPb for BGA256 and BGA196, as shown in Figure 10. The superior drop test performance of SAC-Ti has been studied by Liu et al. [1] and is attributed to (1) the increased grain size & dendrite size, therefore reduced hardness of solder, (2) inclusion of Ti in the IMC layer, and (3) reduced IMC layer thickness. For CSP64, where the solder joint is considerably smaller, and thus may be more sensitive to voiding, the voiding may dictate fracture performance. Table 13 summarizes the relation between pasty range and Ti on fracture performance.

3. Effect of Hot Reflow Temperature

As discussed in the previous section, a high reflow temperature drives the fracture site to shift from resin to solder interface. When the reflow temperature is high enough, such as small package CSP64 with lead-free assembly, the fracture further shifts to the top interface of the solder joint, as shown in Figure 11 to 13. In general, the top interface went through two reflows, one for bumping, and one for assembly. On the other hand, the bottom interface went through one reflow only. It is hypothesized that at sufficiently high reflow temperatures, the IMC thickness at top interface exceeded a threshold value, thus

Table 12 - Gibbs free energy of metal oxide formation at ambient temperature

Metal oxide	$\Delta G°_f$ (KJ/mol)	Metal oxide	$\Delta G°_f$ (KJ/mol)
MgO	-1220	SnO_2	-540
Al_2O_3	-1150	FeO	-480
ZrO_2	-1040	NiO	-460
TiO_2	-880	Cu_2O	-300
MnO	-805	CuO	-127

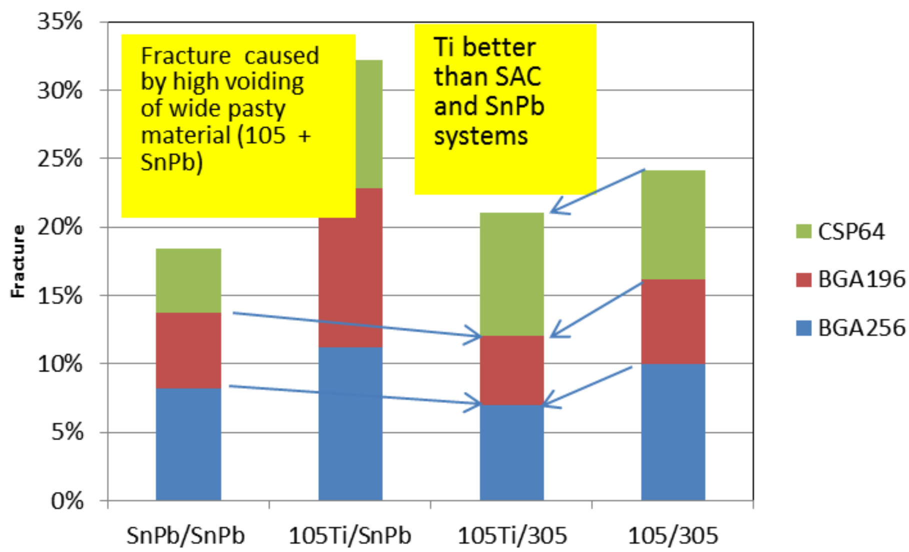

Figure 10 - Effect of alloy combination on fracture

Table 13 – Effect of pasty range and Ti on fracture performance

Package	SnPb/SnPb	105Ti/SnPb	105Ti/305	105/305
BGA256		47C pasty range (177C to 224C), very bad voiding, cause highest failure. Ti oxidation may aggravate	Ti show positive effect despite voiding, except at small joints where voiding dictate.	
BGA196				
CSP64				

became the primary fracture site. Here presence of Ti appears to have negligible effect. Table 14 summarizes the effect of hot reflow temperature on fracture site.

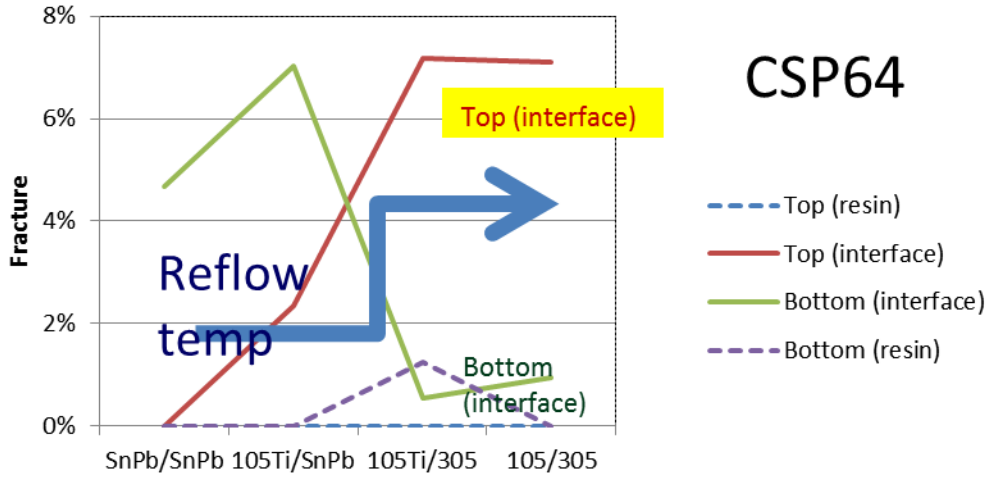

Figure 11 - Relation between reflow temperature and fracture site

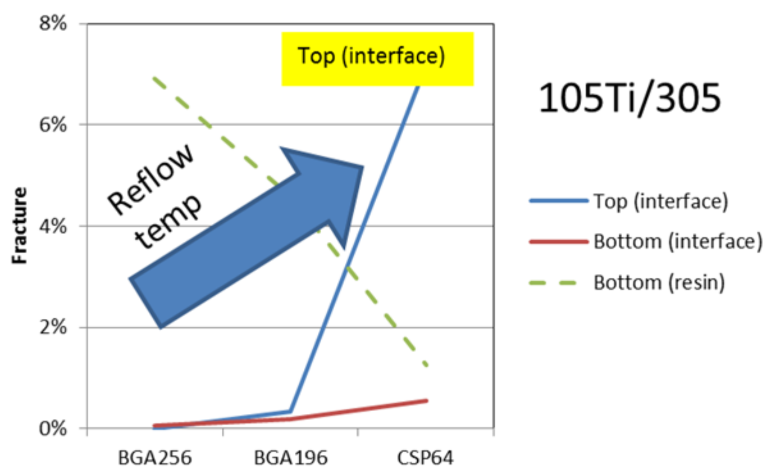

Figure 12 - Relation between reflow temperature and fracture site for 105Ti/305

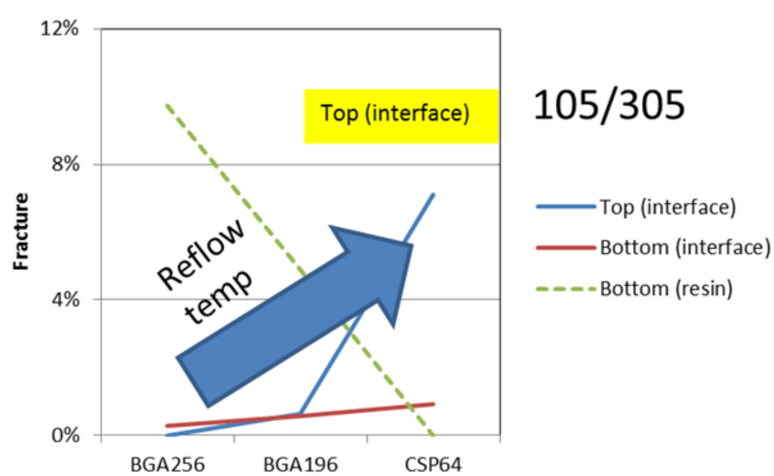

Figure 13 - Relation between reflow temperature and fracture site for 105/305

Table 14 – Effect of hot reflow temperature on fracture site

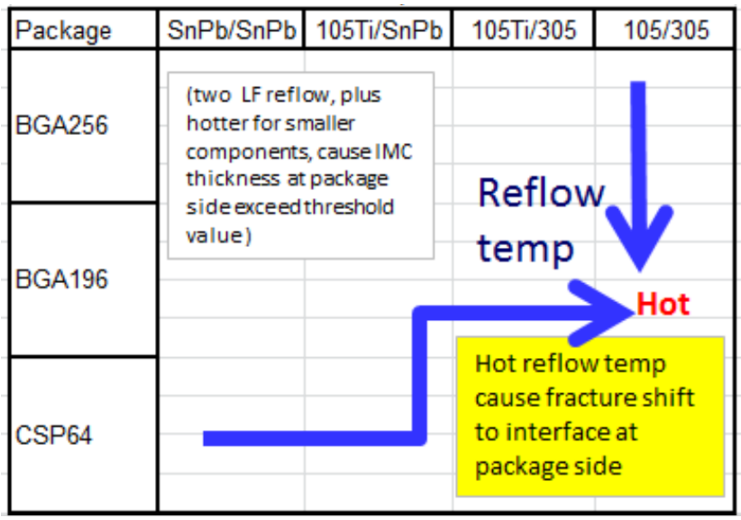

Discussion

The presence of Ti improved the drop test performance significantly, despite the voiding side effect caused by its oxidation tendency. The flux used here is a regular no-clean flux. It is anticipated that the voiding can be prevented with the development of a more oxidation resistant flux. Once developed, the Ti-doped alloy is expected to have an even higher drop test performance.

2. Wide Pasty Range of Mixed Alloys

The consistently poor drop test performance of 105Ti/SnPb is caused by the wide pasty range resulting from mixing SAC105Ti with Sn63 solder paste. The effect of Ti in this system is overshadowed by the high voiding outcome due to this wide pasty range material. In view of this, the use of SAC105 BGA with SnPb solder paste is not recommended, with or without Ti addition.

3. Reflow Temperature

High reflow temperatures shifted the fracture site to the interface at the package side, presumably through building up the IMC thickness beyond the threshold value. A lower reflow temperature is recommended.

4. Virtual Fracture Model

The electrical response is consistent with the complete fracture data, but the complete fracture trend is inconsistent with that of the partial fracture trend, and neither data can provide a full understanding about the failure mode. By integrating the complete fracture and partial fracture into a "Virtual Fracture", the failure mechanism becomes obvious and the data sets become consistent with each other.

Conclusions

Board-level drop test performance was evaluated and compared for the following four different solder combinations in BGA/CSP assembly: 1) SnPb paste with SnPb balls, 2) SnPb paste with SAC105Ti balls, 3) SAC305 paste with SAC105Ti balls, and 4) SAC305 paste with SAC105 balls. The Ti doping improved the drop test performance significantly, despite the voiding side effect caused by its oxidation tendency. It is anticipated that the voiding can be prevented with the development of a more oxidation resistant flux. The consistently poor drop test performance of 105Ti/SnPb is caused by the wide pasty range resulting from mixing SAC105Ti with Sn63 solder paste. The effect of Ti in this system is overshadowed by the high voiding outcome due to this wide pasty range material. In view of this, the use of a SAC105 BGA with an SnPb solder paste is not recommended, with or without the Ti addition. High reflow temperatures shifted the fracture site to the interface at the package side, presumably through building up the IMC thickness beyond the threshold value. A lower reflow temperature is recommended. The electrical response is consistent with the complete fracture data, but the complete fracture trend is inconsistent with that of the partial fracture trend, and neither data can provide a full understanding about the failure mode. By integrating the complete fracture and the partial fracture into a "Virtual Fracture", the failure mechanism becomes obvious and data sets become consistent with each other.

Reference

1. Weiping Liu, Paul Bachorik, and Ning-Cheng Lee, "The Superior Drop Test Performance of SAC-Ti Solders and Its Mechanism", 58th ECTC, Lake Buena Vista, Florida, May 27-30, 2008.

2. G. Henshall et al, "iNEMI Pb-Free Alloy Alternatives Project Report: State of the Industry", Proceedings SMTA International 2008, Orlando, Florida, August 2008.
3. G. Henshall et al., "Addressing Industry Knowledge Gaps Regarding New Pb-Free Solder Alloy Alternatives" Proceedings of 33rd International Electronics Manufacturing Technology Conference 2008.
4. Kanto Yakin Kogyo Co., Ltd, "Free energy of metal oxide formation", 2003, http://www.k-y-k.co.jp/en/graph.html.